Int J Ind Chem (2016) 7:315–331
DOI 10.1007/s40090-016-0092-x

RESEARCH

Effective removal of radioactive ^{90}Sr by CuO NPs/Ag-clinoptilolite zeolite composite adsorbent from water sample: isotherm, kinetic and thermodynamic reactions study

Meysam Sadeghi[1] · Sina Yekta[2] · Hamed Ghaedi[3] · Esmaeil Babanezhad[2]

Received: 4 October 2015 / Accepted: 4 July 2016 / Published online: 18 July 2016

Abstract In this research, the natural zeolite named clinoptilolite (NCp) was considered as an applicable base structure for subsequent preparation and modification by pre-selected chemical agents to use for removal/adsorption goals in progress. To make Na-clinoptilolite form, the mentioned zeolite undergoes variations by treating with NaCl salt. Ion exchange procedure was utilized to imprint silver ions (Ag^{+}) from silver (I) nitrate solution as silver precursor on the modified clinoptilolite zeolite structure to attain Ag-clinoptilolite zeolite. Tenorite (CuO) NPs have been then dispersed and deposited on the external surface of the pre-prepared Ag-clinoptilolite zeolite through impregnation method to prepare the CuO NPs/Ag-clinoptilolite zeolite as a novel composite adsorbent. A series of analyses techniques including SEM-EDAX, XRD and FT-IR were applied for characterization and identification of crystal structure, morphology and elemental composition of the synthesized samples. The removal and adsorption process of radioactive strontium-90 (^{90}Sr) by CuO NPs/Ag-clinoptilolite zeolite composite adsorbent was exploited under various experimental conditions including pH, amount of adsorbent and the contact time at room temperature and the final optimized procedure used for removal of probable presence of ^{90}Sr in water sample of Bushehr city. Adsorption isotherm models including Langmuir, Freundlich, Temkin, D-R, H-J and Hasley have been applied and equilibrium adsorption data was better fitted to the Freundlich, Temkin, H-J and Halsey isotherms. The reaction kinetic information was studied by utilizing pseudo first and second orders, Elovich and Intra particle diffusion kinetic models. The adsorption kinetics is finely described by the pseudo second-order model. The energy of activation E_a calculated using the Arrhenius equation was found to be 44.75 kJ/mol. Further, the evaluation of the thermodynamic parameters such as ΔG^0, ΔH^0 and ΔS^0, denoted that adsorption process of ^{90}Sr was spontaneous and illustrates a chemical adsorption properties and exothermic nature of the adsorption. The obtained results revealed that ^{90}Sr ions were removed by CuO NPs/Ag-clinoptilolite zeolite composite under optimized conditions after 6 h with a yield more than 97 %.

Keywords Radioactive ^{90}Sr · CuO NPs/Ag-clinoptilolite zeolite · Removal and adsorption · Isotherm

Introduction

Liquid radioactive wastes (LRWs) are known as by-products of nuclear activities around the world including; nuclear power plants (NPPs) developments and activities, applications of nuclear fission or nuclear technology, nuclear weapon testing, and other world threatening researches. The entrance and existence of these radioactive wastes into the environment always has recognized as a serious threat for human being and other alive creatures. Radioactive contamination is seriously hazardous and if it comes about to an area, it can cause a real disaster not only for the main area but also for the other parts around its

✉ Hamed Ghaedi
hamedghaedi@gmail.com

[1] Young Researchers and Elite Club, Ahvaz Branch, Islamic Azad University, Ahvaz, Iran

[2] Department of Chemistry, Faculty of Basic Sciences, Qaemshahr Branch, Islamic Azad University, Qaemshahr, Iran

[3] Faculty of Engineering, Bushehr Branch, Islamic Azad University, Bushehr, Iran

district depending on the amount of leaked or released radioactive wastes. Despite the other sorts of pollutants which can be removed or handled entirely in a certain period of time, the radioactive wastes cannot be handled in the same way. Because these radioactive wastes can spread widely in any possible way (air, soil, water, alive tissues) and large number of radioactive elements have years and years of half-life which means they are not going to be neutralized in easy way. Standing still and disintegration for years will go on till complete neutralization comes about. However, due to the wide spread of nuclear power plants and public raised concerns over nuclear safety, the new methods and regulations for monitoring and protection against these wastes are developing by researchers and governments.

For instance after the explosion took place in Fukushima in Japan, power plants accident, the enormous amounts of radioactive hazardous elements found their way to the natural environment and finding the best way to bring the best protection and monitoring service was of great concern [1]. For nuclear facilities, it can be very hazardous if such wastes are not well treated before discharged to the environment. Strontium-90 (^{90}Sr) is an important component of many nuclear wastes and is a high yield fusion product of uranium-235 (^{235}U) [2]. It is relatively short-lived with a half-life of 28.8 years. Its decay product that so called daughter of ^{90}Sr, is yttrium-90 (^{90}Y) isotope which is β^- emitter with half-life of 64 h and decay energy of 2.28 MeV distributed to an electron, an antineutrino and zirconium-90 (^{90}Zr) that is stable [3, 4]. Strontium isotope ^{90}Sr is treated as one of the most dangerous products of nuclear fission for human beings [5, 6].

Radioactive strontium can be replaced instead of calcium in biosphere known as a bone seeker and it can also transfer to human body through food chain in which it has long retention time. ^{90}Sr is taken up via gastrointestinal system and aggregate in the body turning to a part of the bone marrow tissue and hurting blood-producing cells [7]. Also, it can be a cause of leukemia or skeletal cancer. This is because of its chemical propinquity and alkaline earth metallic characteristics. For this reason, its characteristics and migration in the environment are widely studied. Drinking waters and fresh waters usually contain many natural radionuclides; Strontium, tritium, radon, radium and uranium isotopes, etc. In recent years, there has been an increase in the usage of zeolites in different compositions to remove and bury different radio-contaminations [8–12]. Zeolites are porous crystalline structurally—hydrated alumina silicates of group IA and IIA elements such as sodium, potassium, barium, magnesium and calcium. One of the most significant properties of zeolites is their ability to exchange cations. Clinoptilolite (Cp) is one of a very cheap, available and the most abundant natural zeolites is in the chemical class of family of Heulandite (HEU-type), easily obtained from mines, appropriate as a sorbent due to its natural characteristics [13, 14].

The crystal structure of clinoptilolite has 3-dimensional aluminosilicate framework, which specific structure causes the developed system of micropores and channels occupied by water molecules and exchangeable cations. The combination of zeolites and metal oxide nanoparticles renders solid catalysts in which the high surface area of nanoparticles and the absorbent capacity provided by zeolites cooperate to increase the efficiency of the catalytic process [15]. As reported in previous researches, the natural clinoptilolite zeolite shows a high adsorbent capacity for the removal of non-radioactive strontium ions [16, 17]. The procedures for modifying zeolites are usually done by impregnation [18] and ion-exchange [17]. Also, the dispersion of metal oxide nanoparticles onto zeolite depends on the type of metal precursor used and its action during the preparation method. Among metal oxides, tenorite or copper oxide (CuO) nanoparticles actuated our attention due to its low cost and availability of the starting materials and also high certainty and purity compared with other applied metal oxides are the advantages of mentioned reagent [19–21].

Tenorite nanoparticles (NPs) as a p-type semiconductor exhibiting narrow band gap (Eg = 1.2 eV), have attracted a great scope of research interest in this decade. These nanoparticles are also utilized in a wide range of applications such nano devices such as degradation, bactericidal properties, etc. [22–24]. Herein, we will report the combination of Ag-clinoptilolite zeolite as host and CuO nanoparticles as guest materials to synthesize CuO NPs/Ag-clinoptilolite zeolite composite an adsorbent catalyst in which the high surface area of nanoparticles and the absorbent capacity provided by the zeolite cooperation to increase the efficiency of the removal process of radioactive ^{90}Sr from water sample of Bushehr city. Ag^+ is the only noble mono-positive cation that forms mononuclear species with appreciable stability in aqueous solution. Besides, silver is known to have strong influence on the absorption properties of zeolites. To the best of our knowledge, there is no report on the application of CuO NPs/Ag-clinoptilolite zeolite composite catalyst used for the removal of radioactive ^{90}Sr.

Experimental

Materials and reagents

The natural clinoptilolite (NCp) zeolite employed in our research was obtained from the region of the West Semnan, Central Alborz Mountains, Iran and its structural properties

is as (Na, K, Ca)$_6$(Si, Al)$_{36}$O$_{72}$.20H$_2$O. Sodium chloride (NaCl), silver nitrate ($AgNO_3$), hydrochloric acid (HCl), copper nitrate trihydrate ($Cu(NO_3)_2.3H_2O$), acetone, sodium hydroxide (NaOH) and nitric acid (HNO_3) were purchased from Merck (Merck, Darmstadt, Germany). The high-capacity cocktail OptiPhase HiSafe-3 (Wallac Oy, Turku, Finland) and deionized water were used throughout the work.

Instrumentation

The morphology, particle sizes and elemental composition of the prepared adsorbents were surveyed using a scanning electron microscope coupled with energy dispersive X-ray spectrometer (SEM-EDAX, HITACHI S-300 N). The powder X-ray diffraction (XRD) patterns were recorded using a Philips X'pert Pro diffractometer equipped with CuKα radiation at wavelength 1.54056 Å (30 mA and 40 kV) at room temperature. Data were collected over the range 4–80° in 2θ with a scanning speed of 2° min^{-1}. The IR spectra were scanned on a PerkinElmer model 2000 FT-IR spectrometer (USA) in the wavelength range of 400–4000 cm^{-1} using KBr pellets. An ultra low-level Quantulus 1220 liquid scintillation counter has been used for all measurements. A shaker Heidolph Vibramax 100 (Heidolph Co., Schwabach, Germany) was utilized for mixing of cocktail and sample. The samples and cocktail were mixed in 20 mL polyethylene vials, Polyvial (Zinsser Analytik Co., Frankfurt, Germany).

Preparation of Na-clinoptilolite zeolite

First, 5 g of the clinoptilolite zeolite before processing was calcined at 300 °C for 2 h in a furnace for excluding moister and impurities from the surface. Then, to obtain the Na-clinoptilolite form, the calcined clinoptilolite was chemically treated with 250 ml of 1 M sodium chloride (NaCl) at 90 °C for overnight and was washed with deionized water several times until chloride ions were removed. Finally, treated clinoptilolite (sodium-clinoptilolite) was dried at 85 °C for 5 h [25].

Preparation of Ag-clinoptilolite zeolite

Silver ions were loaded into the zeolite framework by ion exchange method. In a typical experimental procedure, 4.5 g of the prepared Na-clinoptilolite zeolite in the previous step was added to a 50 mL of a 0.1 M silver nitrate ($AgNO_3$) solution and the mixture was magnetically stirred at 60 °C for 5 h to perform ion exchange process in which Ag^+ ions were replaced with Na^+ ions. The synthesized product (Ag-clinoptilolite zeolite) was then filtered and washed with deionized water and 0.1 M HCl solution, to remove the excess and unreacted silver ions from the zeolite framework, sequentially and then dried at 110 °C for 16 h. At last, the clean and dry Ag-clinoptilolite zeolite was calcined at 400 °C for 4 h [26]. This process was repeated for three times to reach significant ion exchange.

Preparation of CuO NPs/Ag-clinoptilolite zeolite composite

Preparation of CuO NPs/Ag-clinoptilolite zeolite composite has been achieved using impregnation method. Typically, 3.5 g of the Ag-clinoptilolite zeolite powder was added to a solution of 0.5 M of copper nitrate trihydrate ($Cu(NO_3)_2.3H_2O$) reagent in 250 mL deionized water, meanwhile, the suspension was vigorously stirred at room temperature for 6 h. When the reaction was completed, the green powders were filtered, washed with distilled water and dried overnight at 110 °C. Finally, the obtained powder was revealed as the CuO NPs/Ag-clinoptilolite zeolite composite after calcination at 500 °C in the air for 6 h [27]. On the other hand, pure CuO NPs was prepared but without the presence of zeolite under similar conditions.

Removal of radioactive ^{90}Sr from water sample by CuO NPs/Ag-clinoptilolite composite

The measuring of probable presence of radioactive ^{90}Sr in water sample needs another independent chemical experiment and the polluted water sample can be examined and monitored before and after removal process via Ultra Low-Level Liquid Scintillation Counting (LSC) technique. To study the removal and adsorption of radioactive ^{90}Sr, amounts of 0.5–3 g of the CuO NPs/Ag-clinoptilolite zeolite composite was added to 500 ml of the water sample. A tracer amount of $^{90}Sr^{2+}$ containing 533 μL amount of it (equal to 112.3 Bq(Becquerel)/L) as the optimized activity was added to the above solution samples. Next, the mixture was stirred in different pH ranges 2–12 and time intervals 1–12 h via varying the adsorption temperature at 298–323 K, respectively. After filtration of the mixture, 5 mL of supernatant solutions were analyzed by liquid scintillation spectrometry (LSC) instrument. In LSC, an aliquot of the sample is put into a vial and mixed homogeneously with 15 mL of scintillation cocktail. A shaker was utilized for mixing of cocktail and sample. The samples and cocktail were mixed together in 20 mL polyethylene vials, Poly vial. The outside of the vials was cleaned with acetone. In the next step, all the polyethylene vials were stored in a cool, dark shield (about 7 °C) for 2 h to eliminate the scintillation cocktail fluorescence. Finally, all samples were counted by LSC for 5 h. The relative error of radioactivity measurements did not exceed 2 %. The initial source activity was 210.8 Bq/L.

Results and discussion

SEM-EDAX analysis

To establish the morphology and crystalline size of the as-synthesized clinoptilolite zeolite, Ag-clinoptilolite zeolite, CuO NPs/Ag-clinoptilolite zeolite composite and pure CuO NPs, SEM analysis were utilized as depicted in Fig. 1. The SEM images explain homogenous morphology of the structures of clinoptilolite (1a) and Ag-clinoptilolite (1b and 1c) zeolites and quasi-spherical CuO nanoparticles dispersed and deposited on the external surface of Ag-clinoptilolite zeolite (1d and 1e) and also specify that these morphologies and the crystallinity of the structures are maintained with Ag ion exchange and CuO NPs loading processes which are indicated by SEM images in Fig. 1b–e. The average crystalline size of CuO NPs in the composite was illustrated to have nanometric dimensions (less than 100 nm). It also denote that CuO NPs loaded on the zeolite has lower crystalline size than that of pure CuO NPs. Figure 2 give the composition elements present in clinoptilolite, Ag-clinoptilolite zeolites, CuO NPs/Ag-

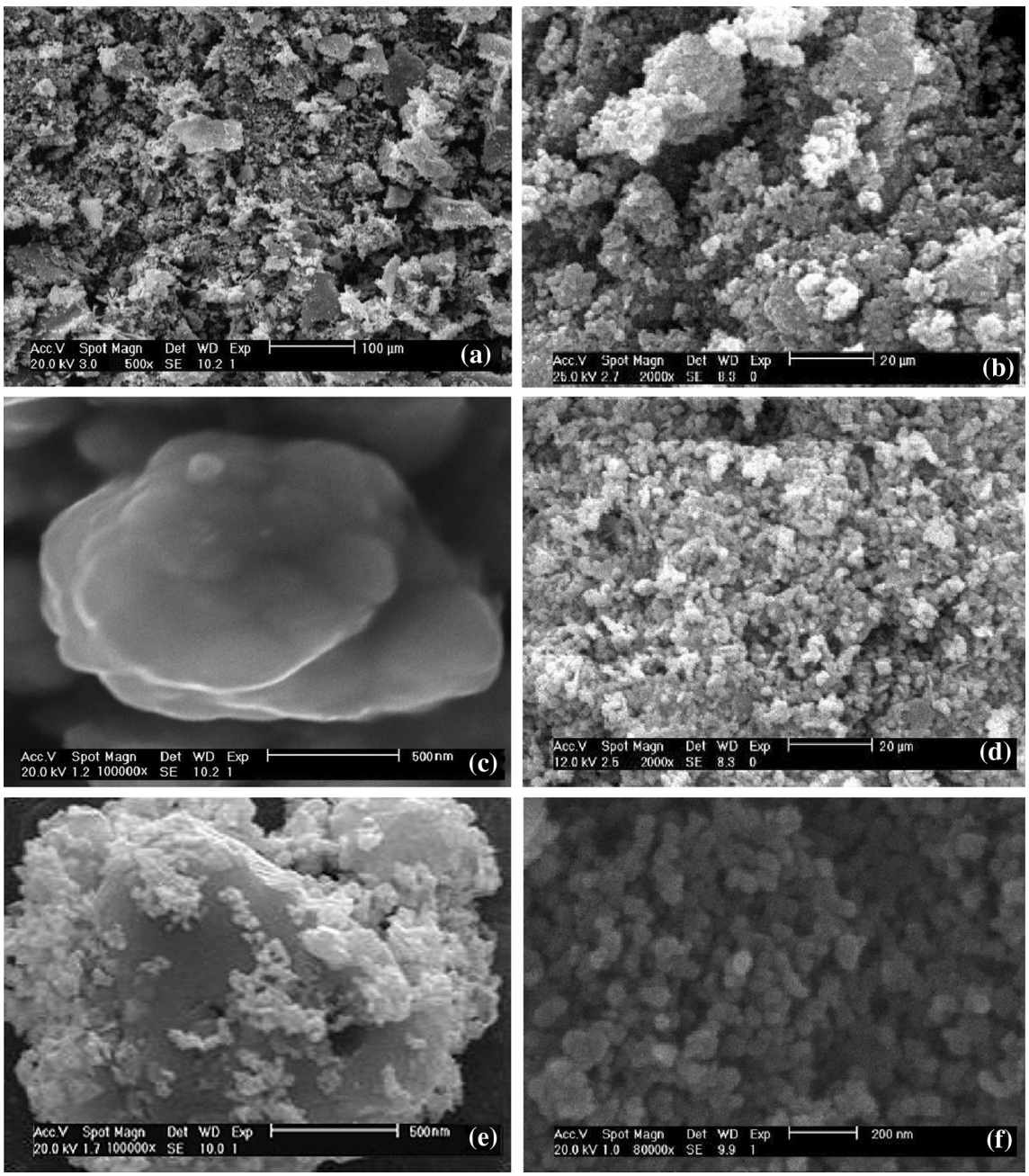

Fig. 1 SEM images of the: **a** clinoptilolite, **b**, **c** Ag-clinoptilolite, **d**, **e** CuO NPs/Ag-clinoptilolite, and **f** pure CuO NPs

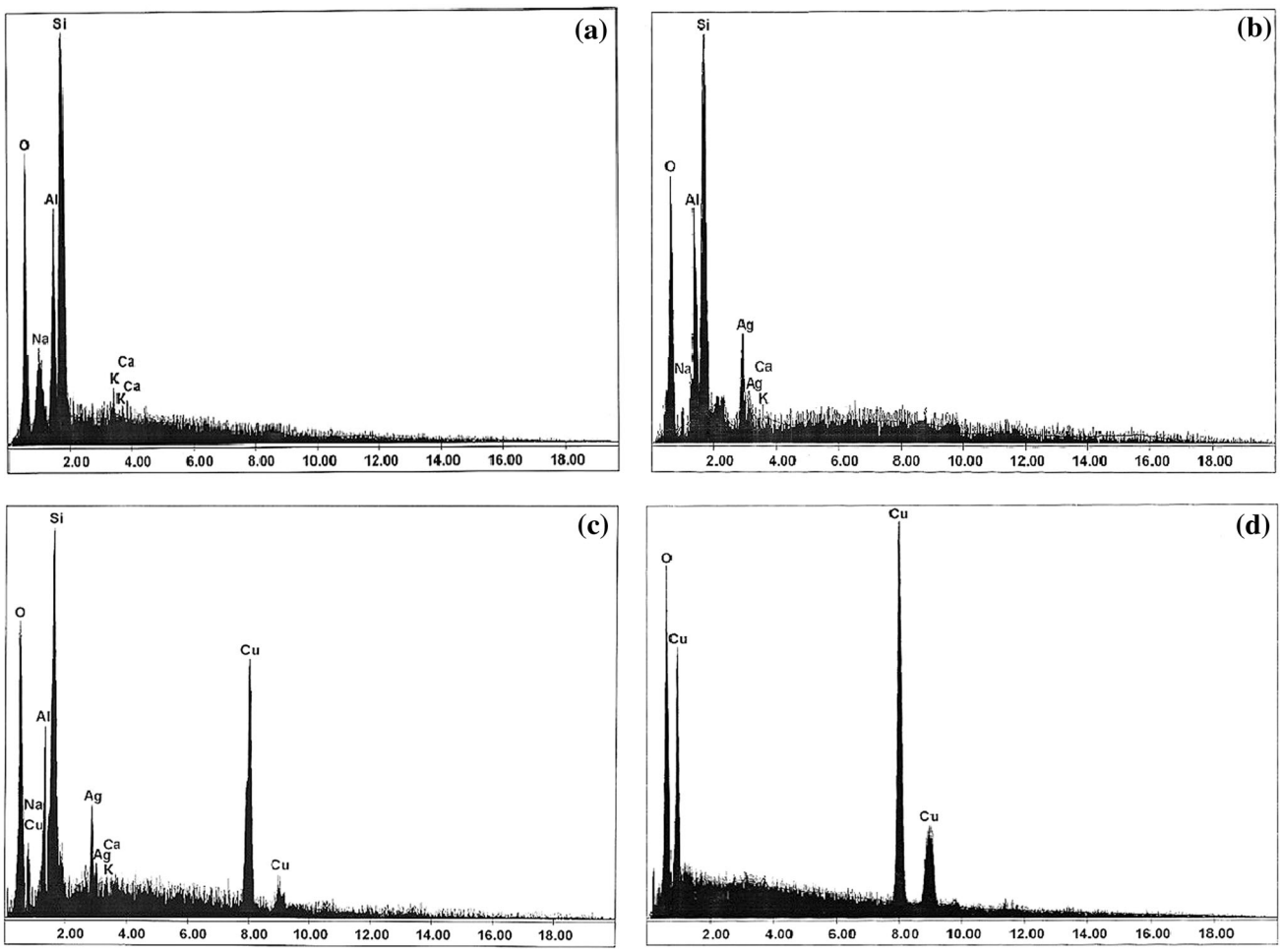

Fig. 2 EDAX analysis of the **a** clinoptilolite, **b** Ag-clinoptilolite, **c** CuO NPs/Ag-clinoptilolite, and **d** pure CuO NPs

clinoptilolite zeolite and CuO NPs were investigated by energy dispersive X-rays (EDAX) analysis. In the EDAX spectra, the appeared peaks in the regions of approximately 0.55, 1.15, 1.50 and 1.75 are corresponded to the binding energies of oxygen (O), sodium (Na), aluminum (Al) and silicon (Si), respectively, that are related to the major elements of the clinoptilolite zeolite (Fig. 2a). On the other hand, in spectra (Fig. 2b, c), the appeared two peaks in the regions of 2.92 and 3.21 keV referred to the binding energies of silver (Ag) and three peaks in the regions of 0.93, 8.04 and 9.03 keV are related to the binding energies of copper (Cu) which reveals the presence of Cu in the composite. These results confirm coexistence of 6.4 and 19.7 wt% silver and copper in the prepared composite network, respectively.

X-ray diffraction (XRD) patterns

In Fig. 3, XRD patterns of the understudy clinoptilolite zeolite, CuO NPs/Ag-clinoptilolite zeolite composite and pure CuO NPs are given, respectively. As seen from the patterns, the sharp peaks referring to clinoptilolite zeolite occurred at (2θ) of 11.3993°–74.1895° (Fig. 3a) and are in good agreement with those of the clinoptilolite zeolite with Joint Committee on Powder Diffraction Standards: (JCPDS: 00-025-1349). Clinoptilolite zeolite structure was retained even after silver cation exchange in the Ag-clinoptilolite (Fig. 3b). Meanwhile, synthesized CuO NPs (as guest material) loaded as a 19.7 wt% of unit onto Ag-clinoptilolite zeolite as the host material, possesses a series of new peaks which were obtained at 2θ of 41.5762°, 45.3174°, and 57.2960° corresponding to the diffraction planes of (002), (111) and (202), respectively [27–30]. No characteristic peaks related to the presence of impurities were observed in the patterns during CuO species loading. These peaks which are illustrated as purple points in Fig. 3b reveal that CuO NPs have been dispersed and deposited onto Ag-clinoptilolite and also indicate a host–guest interaction between Ag-clinoptilolite framework and CuO NPs. A definite line broadening of the scattering pattern in Fig. 3b is a demonstration upon which the synthesized CuO particles are in nanoscale range. However, a

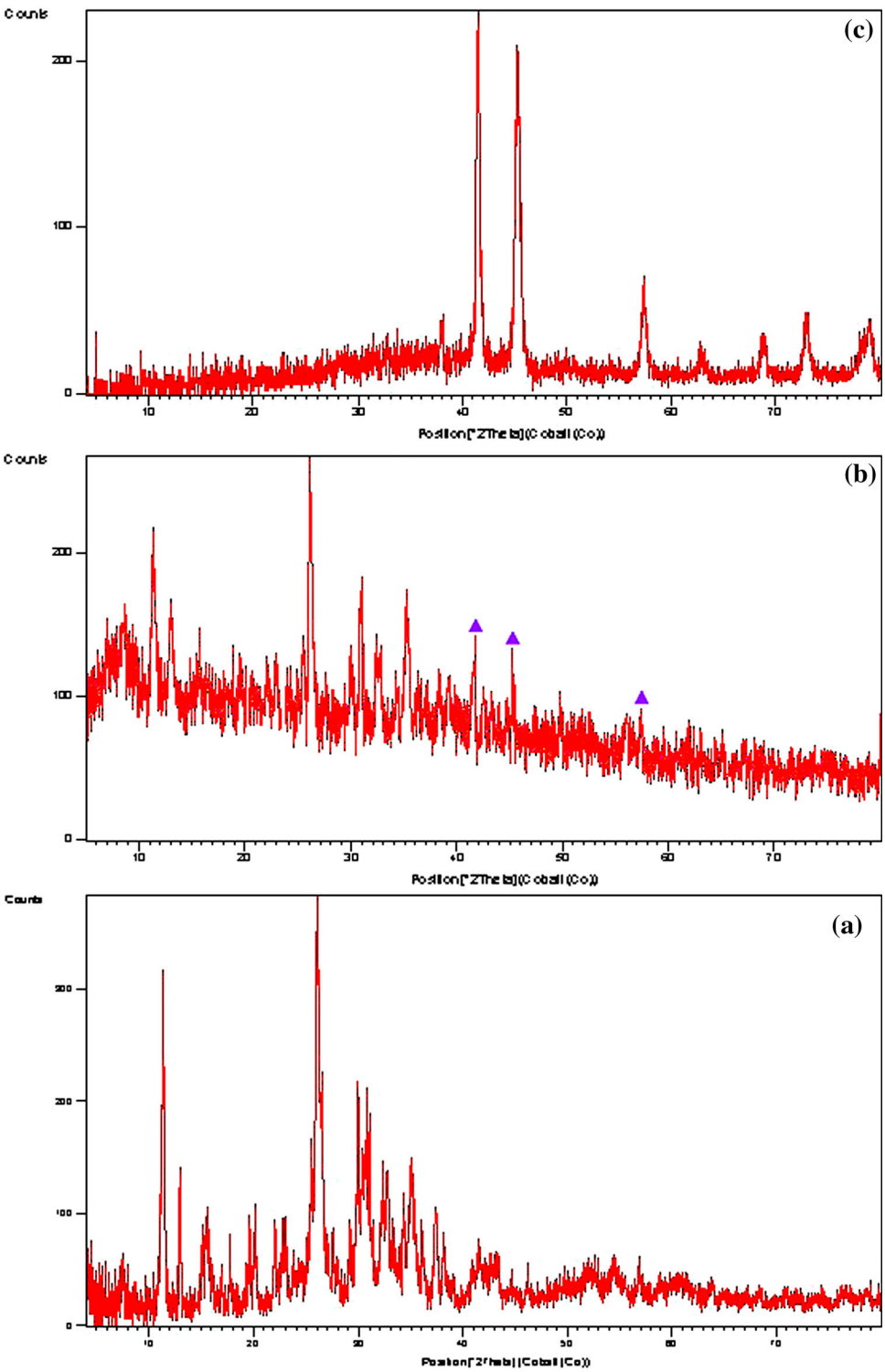

Fig. 3 XRD patterns of the catalyst samples: **a** clinoptilolite, **b** CuO NPs/Ag-clinoptilolite, and **c** pure CuO NPs (*violet color filled triangle* indicates peak pattern depicting presence of CuO in the zeolite framework)

small loss of crystallinity is observed in Fig. 3b associated with the lower intensity of the peaks at 2θ of 11.630° and 18.318°. This may be due to the dealumination process of Ag-clinoptilolite zeolite and CuO NPs/Ag-clinoptilolite zeolite composite and associated with the location of substituted silver and impregnated copper cations. The Cu^{2+} ions within the zeolite framework can interact with the aluminate sites more strongly than that of Na^{+} or Ag^{+} ions. Totally, it can be concluded that with silver ion exchange in clinoptilolite zeolite and subsequent loading of CuO NPs onto Ag-clinoptilolite, the structure of the zeolites did not change and can be stable after the above processing. On the other hand, the capacity of the clinoptilolite zeolite to keep the guest species is certainly limited. Consequently, the

adsorption of the host cations (Si, Al and Na) will stop if the capacity is saturated. In contrast, the amount of the host species in the Ag-clinoptilolite increases as the copper oxide content increases. The introduced CuO NPs were dispersed and deposited on the external surface of Ag-clinoptilolite, however, due to the relative aggregation during processing of the composite, some particles are too large to perch inside the structure. Hence, high CuO NPs loading will cause structural damage to the zeolite framework. The size of the prepared CuO NPs deposited onto Ag-clinoptilolite was also investigated via XRD measurement and line broadening of the peak at $2\theta = 0°$–$80°$ using Debye–Scherrer Eq. (1) [31]:

$$d = \frac{0.94\lambda}{\beta \cos\theta}, \tag{1}$$

where d is the crystal size, λ is the wavelength of X-ray source, β is the full width at half maximum (FWHM) and θ is Bragg diffraction angle. The peaks referring to the pure CuO NPs (Fig. 3c) occurred at scattering angles (2θ) of 37.9379°, 41.5859°, 45.3296°, 57.3058°, 62.9655°, 68.9326°, 72.9516° and 78.8583° corresponding to diffraction planes of (100), (002), (111), (202), (113), (220), (311), and (222), respectively, that have been crystallized in the monoclinic phase and are in good agreement with those of CuO NPs with JCPDS = 01-072-0629. Using this equation, the average particle size for CuO NPs in the CuO NPs/Ag-clinoptilolite zeolite composite and pure CuO NPs are estimated to be 8.3 nm and 37.6 nm, respectively. The particle size obtained from XRD measurement is consistent with the results from the SEM study.

FTIR study

The characterization of the prepared adsorbents along with the clinoptilolite zeolite precursors were further surveyed by FT-IR spectra as plotted in Fig. 4. Peak positions are nearly identical for three samples. All of the three as-synthesized typical samples, namely clinoptilolite zeolite and CuO NPs/Ag-clinoptilolite zeolite composite have peaks around 465 cm^{-1} and 524 cm^{-1} which are assigned to the bending vibrations of the insensitive internal TO_4 (T = Si or Al) tetrahedral units and double six rings (D6R) external linkage within the clinoptilolite zeolite structure, respectively. The peaks around 674 cm^{-1} and 797 cm^{-1} are attributed to the external linkage and internal tetrahedral symmetrical stretching vibrations, respectively. Furthermore, the peaks around 1034 cm^{-1} are corresponded to the external linkage and internal tetrahedral asymmetrical stretching vibrations, and peaks around 1635 cm^{-1}, 3437 cm^{-1} and 3623 cm^{-1} are attributed to H–O–H bending O–H bonding (hydroxyl groups) vibrations and discrete water absorption bands of the clinoptilolite, respectively. Surveying Fig. 4a, b confirms that no changes has occurred in the bands of Ag-clinoptilolite zeolite and CuO NPs/Ag-clinoptilolite zeolite composite compared with the original clinoptilolite zeolite, which tends to lend further support to the idea that the ion exchange modification of clinoptilolite zeolite by silver ion and copper oxide has a very little influence on the chemical structure of the zeolite framework. On the other hand, Fig. 4b illustrates two new peaks related to the synthesized loaded CuO NPs. The absorption bands in the 1467 cm^{-1} region is referred to C–C bonding of probable trivial impurities existing in the applied stock materials. The absorption peak at 967 cm^{-1} is also corresponded to Cu–O–Si and Cu–O–Al bonds and revealed the entrapped copper in the structure of zeolite [26–28]. Also, Fig. 4c reveals the FT-IR spectrum of pure CuO NPs. The broad at absorption peak around 3441 and 1632 cm^{-1} were caused via the adsorbed water molecules. The absorption bands in the 1461 cm^{-1} region is probably related to C–C bonding of trivial impurities existing in the applied stock materials as implied above. Three peaks at 487, 523 and 580 cm^{-1} were related to the stretching vibrations of Cu–O bonding.

Adsorption reaction isotherms

Several adsorption isotherm models were developed via analyzing solutions in contact with CuO NPs/Ag-clinoptilolite zeolite composite to find out the relation between the equilibrium concentrations before and after experimental in the liquid and solid phases. The Langmuir, Freundlich, Temkin, Dubinin–Radushkevich (D–R), Harkins–Jura (H–J) and Hasley models are used to describe equilibrium adsorption isotherms. The sorption isotherms were studied in water sample of Bushehr city as pH = 8.5, temperature (25 °C), and different initial solution concentrations related to the seven various activity of ^{90}Sr from 112.3 Bq/L to 180.6 Bq/L. As can be seen in Fig. 5, by increasing the activity of solution, the removal efficiency of ^{90}Sr is decreased. Thus, activity equal to 112.3 Bq/L as optimized activity for the adsorption reaction was chosen.

This model supposes that the adsorption takes place at a specific adsorption surface. The attraction between molecules decreases as they are getting further from the adsorption surface. The Langmuir adsorption isotherm is often utilized to describe the maximum adsorption capacity of an adsorbent and also show single coating layer on adsorption surface. Langmuir isotherm can be defined according to the following Eq. (2) [32].

$$\frac{1}{q_e} = \frac{1}{K_L q_m} \times \frac{1}{C_e} + \frac{1}{q_m} \tag{2}$$

where q_m and q_e are the maximum and equilibrium uptake of ^{90}Sr per unit mass of adsorbent (mg/g), respectively. Also K_L and C_e refer to the Langmuir constant and the

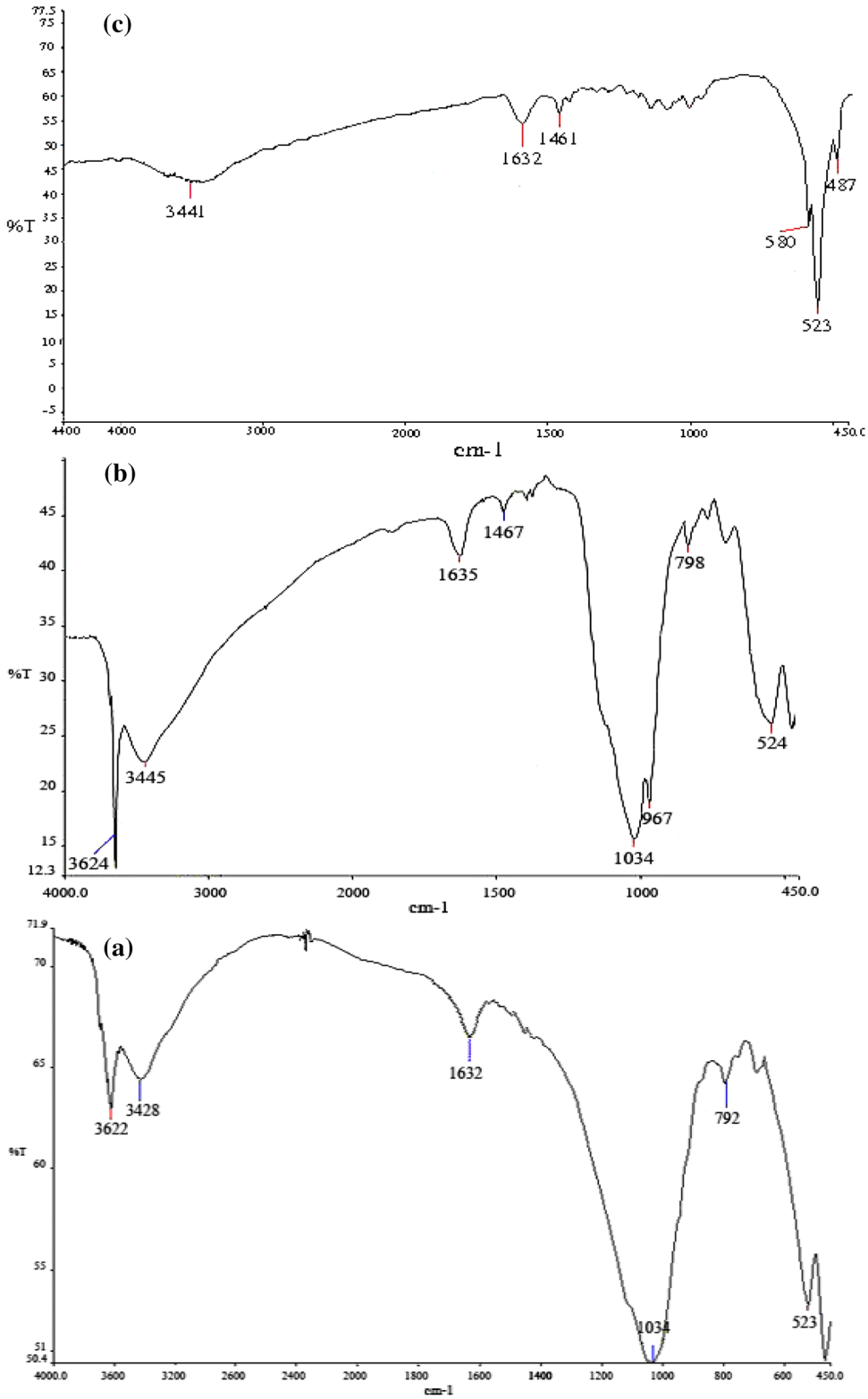

Fig. 4 FTIR spectra of the catalyst samples: **a** clinoptilolite, **b** CuO NPs/Ag-clinoptilolite, and **c** pure CuO NPs

equilibrium concentration of the adsorbent, respectively. The plot corresponded to $\frac{1}{q_e}$ versus $\frac{1}{C_e}$ was depicted and all affiliated data applied in Table 1. Moreover, the plot of q_e versus C_e is shown in Fig. 6 in below.

The Freundlich isotherm is often used for modeling the multilayer adsorption on heterogeneous surfaces and also applied for the very low concentration. It suggests that sorption is not restricted to one specific class of the sites

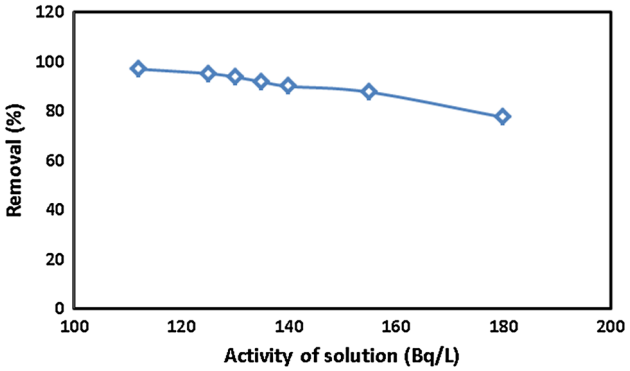

Fig. 5 The effect of solution activity on the removal efficiency of ^{90}Sr by CuO NPs/Ag-clinoptilolite zeolite ($T = 25$ °C, pH: 8.5, amount of adsorbent: 1.5 g, contact time: 6 h)

and assumes surface heterogeneity. This isotherm can be explained by the following Eqs. 3 and 4 [33]:

$$q_e = K_f C_e^{\frac{1}{n}} \tag{3}$$

$$\ln q_e = \ln K_f + \frac{1}{n} \ln C_e \tag{4}$$

where K_f (mg/g) and n are Freundlich adsorption constants that were determined from the intercept and slope of the plot. The plot of this isotherm gives a straight line of slope ln q_e versus ln C_e.

The Temkin isotherm suggests a linear decease of sorption energy and can be expressed via the following Eq. (5) [34]:

$$q_e = \beta \ln \alpha + \beta \ln C_e \tag{5}$$

Here α and β are Temkin adsorption constants. The plot of this isotherm shows a straight line of slope q_e versus ln C_e.

The Dubinin–Radushkevich (D–R) can be simplified to the following equations below (6 and 7) [35]:

$$\ln q_e = \ln q_m - K\varepsilon^2 \tag{6}$$

$$\varepsilon = RT \ln\left(1 + \frac{1}{C_e}\right) \tag{7}$$

where q_m and K are Dubinin–Radushkevich adsorption constants that were calculated from the intercept and slope of the plot. K is the adsorption energy. q_m is the theoretical saturation capacity and ε is the polanyi potential. The plot of this isotherm gives a straight line of slope ln q_e versus ln C_e.The Harkins–Jura (H–J) isotherm can be defined to the following Eq. (8) [35]:

$$\frac{1}{q_e^2} = \left(\frac{B_{HJ}}{A_{HJ}}\right) - \left(\frac{1}{A_{HJ}}\right) \ln C_e \tag{8}$$

where A_{HJ} is the Harkins–Jura isotherm parameter which accounts for multilayer adsorption and explains the existence of heterogeneous pore distribution in which B_{HJ} is the isotherm constant. The plot of this isotherm gives a straight line of slope ln q_e versus ln C_e.

The Hasley isotherm model can be utilized to evaluate the multilayer adsorption for the adsorption of ^{90}Sr at a relatively large distance from the surface. Herein we discuss this isotherm model with equilibrium equation below (9) [36]:

$$\ln q_e = \left[\left(\frac{1}{n_H}\right) ln(K_H)\right] - \left(\frac{1}{n_H}\right) \ln\left(\frac{1}{C_e}\right) \tag{9}$$

n_H and K_H parameters are Hasley isotherm constants and were calculated from the slope and intercept of the linear plot based on ln q_e versus ln$\left(\frac{1}{C_e}\right)$ respectively.

The conformity between experimental data and the model predicated values was expressed by the correlation coefficient (R^2). A relatively high R^2 value reveals that the model successfully describes the adsorption isotherm. It is obvious that the Langmuir and D–R isotherm models cannot correlate the experimental data well. Based on the

Table 1 Various adsorption isotherm model parameters results for removal and adsorption of ^{90}Sr by CuO NPs/Ag-clinoptilolite zeolite composite ($T = 25$ °C, pH: 8.5, amount of adsorbent: 1.5 g, contact time: 6 h)

Isotherm type	Isotherm parameters		Plot equation
Langmuir	$K_L = 6\times10^{12}$ (L/mg) $q_m = 0.1667 \times 10^{-5}$ (mg/g)	$R^2 = 0.8662$	1×10^{-5}x + 6×10^{7}
Freundlich	$K_f = 2.62 \times 10^{6}$ (mg/g) (L/mg) $n = 8.510$	$R^2 = 0.9783$	0.1175×-14.781
Temkin	$\alpha = 1.586 \times 10^{15}$ (g/mg) $\beta = 2\times10^{-9}$ (mol^2/KJ^2)	$R^2 = 0.9737$	$2 \times 10^{-9} \times +2 \times 10^{-8}$
D–R	$K = 2\times10^{-10}$ (L/mg) $q_m = 2.87 \times 10^{7}$ (mg/g)	$R^2 = 0.8256$	$2 \times 10^{-10} \times -17.174$
H–J	$A_{HJ} = 1.11 \times 10^{-15}$ (L/mg) $B_{HJ} = 2220$	$R^2 = 0.9759$	$-9 \times 10^{14} \times -2 \times 10^{16}$
Hasley	$n_H = 8.510$ $K_H = 4.26 \times 10^{54}$ (L/mg)	$R^2 = 0.9783$	-0.1175×-14.781

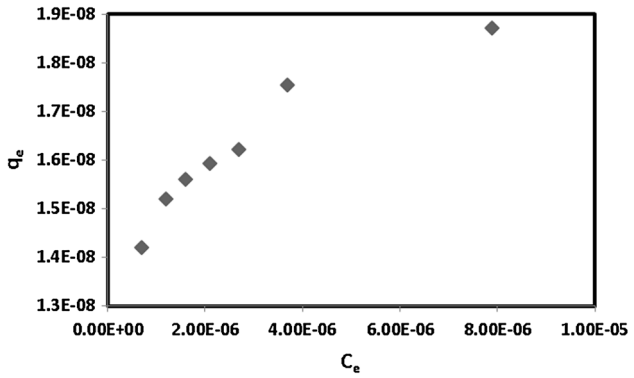

Fig. 6 The plot for the adsorption of ^{90}Sr by CuO NPs/Ag-clinoptilolite zeolite composite ($T = 25$ °C, pH: 8.5, amount of adsorbent: 1.5 g, contact time: 6 h)

R^2 value, high regression correlation coefficient was found in good straight linear with the Freundlich ($R^2 = 0.9783$), Hasley ($R^2 = 0.9783$), H–J ($R^2 = 0.9759$) and Temkin ($R^2 = 0.9737$) isotherms as compared to the Langmuir ($R^2 = 0.8662$) and D–R ($R^2 = 0.8256$) isotherm models. The obtained data from these models are summarized in Table 1.

Removal and adsorptive properties study

Various radiometric methods such as gas flow GM (Geiger–Müller) counting and liquid scintillation counting are usually used for direct measurement of ^{90}Sr and its daughter ^{90}Y subsequently. Ultra low-level liquid scintillation counting (LSC) can be successfully utilized for counting alpha and beta activity derived from alpha, beta emitters to monitor the natural radioactivity, contamination related to nuclear fall-outs, contaminants branched from nuclear power stations or fuel reprocessing plants. Reduced equipment requirements and relative readiness of radiochemical procedures make LSC an attractive technique which can be applied also by laboratories lacking specific radiochemistry facilities and experience. The determination of radiostrontium by this technique is based on the high counting efficiency for high-energy β-particles in aqueous solutions [37]. To evaluate the removal of radioactive ^{90}Sr, the adsorption behavior of CuO NPs/Ag-clinoptilolite zeolite composite was assessed and those progresses were monitored by LSC instrument. The effects of several operational parameters such as pH, amount of adsorbent and contact time, and also kinetics and thermodynamic reactions were considered.

Effect of pH

The effect of initial pH parameter on the removal and adsorption of radioactive Sr^{2+} ions by CuO NPs/Ag-clinoptilolite zeolite composite has been investigated. The role of pH on the removal and adsorption yield of CuO NPs/Ag-clinoptilolite zeolite adsorbent was surveyed via utilizing ^{90}Sr solution of 112.3 Bq/L at optimized temperature (25 °C) for 6 h. As represented in Fig. 5, the adsorption characteristics of ^{90}Sr were investigated in pH ranges 2–12 on the removal of ^{90}Sr by CuO NPs/Ag-clinoptilolite zeolite composite. As pH was increased above pH 2, the percentage removal process of strontium increased in an approximately linear fashion up to a maximum value at about pH 8.5. Therefore, in the pH range of 2–8.5 strontium exists in the form of Sr^{2+} and in high pHs (above 10) it can be found as $Sr(OH)^+$. Plus, when pH is low (pH 2 or less) no more affinity between the adsorbent and Sr^{2+} ions can be observed. Besides, high acidity will lead to replacement of adsorbed Sr^{2+} by H^+ from the solution and decrease the adsorption/removal efficiency as a result [38]. To gain the most selectivity and removal efficiency, pH of 8.5 was considered for the further modifications and more than 97 % adsorption yield. The solution pH was adjusted via 1 M solutions of NaOH and HNO_3. Moreover, the sorption equilibrium was achieved, the supernatant solution of ^{90}Sr were brought out and introduced to the Ultra Low-Level Liquid Scintillation Counter (LSC). Subsequently, the removal and adsorption value percentage of ^{90}Sr by composite adsorbent was calculated. The interaction of hydrogen ions with an oxygen radical of the CuO NPs/Ag-clinoptilolite zeolite composite body generates hydroxyl groups and lowers the charge of the matrix, which is accompanied by a decrease in the sorption ability of CuO NPs/Ag-clinoptilolite zeolite composite in relation to ^{90}Sr. Besides, a higher sorption of the radioactive due to increasing pH shows that in the solution they are in an ionic state.

Effect of amount of adsorbent

Selecting the desirable amounts of adsorbent is a key parameter which obviously affects the whole removal procedure. The adsorption characteristic of ^{90}Sr was investigated at scope of 0.5–3 g of composite adsorbent to recognize the best and optimized amount of adsorbent for the removal of ^{90}Sr. The obtained results revealed that the more the adsorbent amount, the better the removal efficiency, until the point after which no more significant variations is seen and the curve slope tend to a linear form which means constant values. Hence, the value of 1.5 g was chosen as the appropriate mass for CuO NPs/Ag-clinoptilolite zeolite composite to fulfill high yield removal and adsorption.

Effect of contact time

To provide a perspicuous comparison between removal and adsorption capability of CuO NPs/Ag-clinoptilolite zeolite

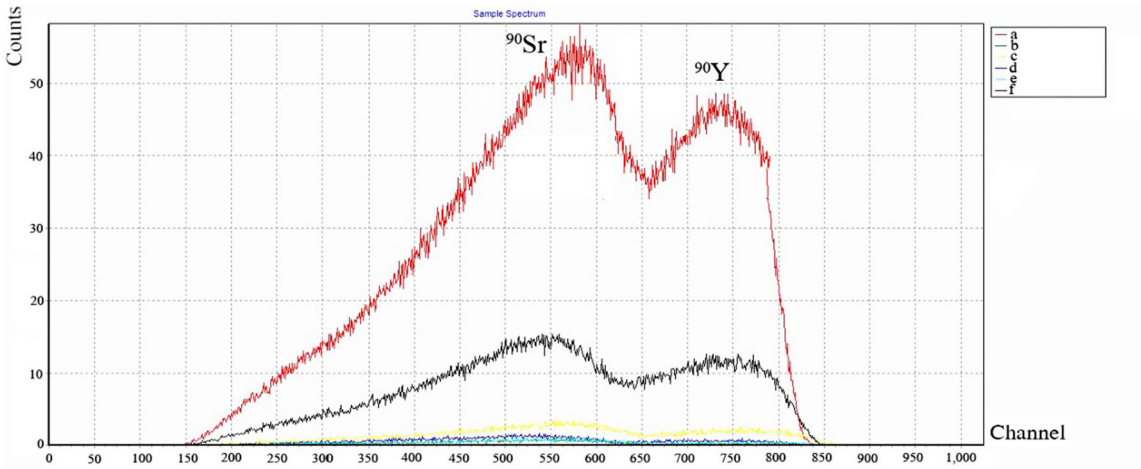

Fig. 7 Liquid scintillation counting (LSC) spectra for removal of ^{90}Sr (count versus channel); **a** before contacting with composite, **b** 1 h, **c** 3 h, **d** 6 h, **e** 9 h and **f** 12 h, under optimized conditions (pH = 8.5, temperature (T = 25 °C) and amount of adsorbent (1.5 g))

composite and reaction time, the effect of different contact time intervals on the adsorption process of ^{90}Sr was accomplished. The spectra of ^{90}Sr/^{90}Y and related results have been presented in Figs. 7, 8, and Table 2, respectively. The variation of adsorption value (%) with shaking time has been shown in Fig. 8. Figure 8 represents the reliability of adsorption yield of ^{90}Sr on the composite adsorbent to the contact time. As the reaction time increases, the adsorption will increase scarcely. On the other hand, rate of counts per minutes (CPM) from 45,065 and 3959 decreases up to 1272 and 118 counts per minutes (CPM), respectively. The similar results are seen in previous researches [39, 40]. The adsorption time was investigated in the scope of 1–12 h, and LSC spectra analysis revealed that the removal first enhanced up to 6 h and then remained in constant value. Thereupon, to reach a shorter analysis period of time 6 h was considered as optimum value. The obtained results from designed experiment revealed that the sorption procedure was rapid and

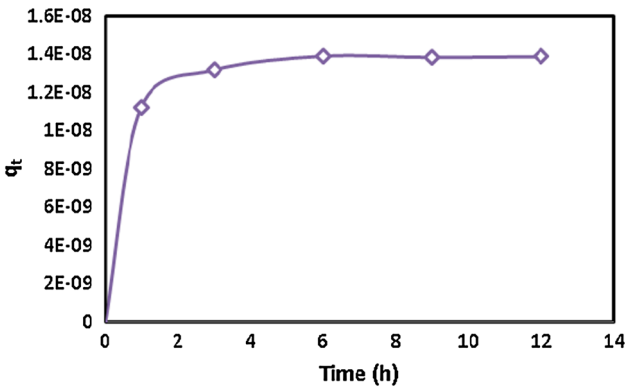

Fig. 8 The effect of contact time on the removal efficiency of ^{90}Sr by CuO NPs/Ag-clinoptilolite zeolite (T = 25 °C, pH: 8.5, amount of adsorbent: 1.5 g)

equilibrium attained quickly after roiling the composite adsorbent with target containing solution. ^{90}Sr uptake on the CuO NPs/Ag-clinoptilolite zeolite composite may be the cause of vicissitude of target metallic ion with the other ions presented on the adsorbent surface area. The Determination of the activity of ^{90}Sr was accomplished using the double-energetic windows method. The energetic window A (150–760) contains all the ^{90}Sr spectrum and low energy region of ^{90}Y spectrum. The window B (760–940) contains the high-energy region of the ^{90}Y spectrum. ^{90}Sr analysis of natural water sample from the Bushehr city of Iran was considered. The removal efficiency was also computed using the following Eq. (10):

$$R(\%) = \left(\frac{A_0 - A_e}{A_e}\right) \times 100 \tag{10}$$

where A_0 is the initial radioactivity and A_e is the radioactivity of ^{90}Sr at equilibrium after sorption process. The minimum detectable activity (MDA) was evaluated using Currie formula (11) and (12) as can be seen in below [41]:

$$\text{MDA}\left(\frac{Bq}{\text{kg}}\right) = L_d(\varepsilon TQ)^{-1} \tag{11}$$

$$L_d(\text{counts}) = 2.71 + 4.65(BT)^{-1.2} \tag{12}$$

where ε is the detection efficiency; T is the counting time (s); Q is the sample quantity (kg); B is the background count rate (s^{-1}).

The following formula can be used for the conversation of strontium-90 activity it's mass in gram (13):

$$M = \frac{A \times T_{\frac{1}{2}} \times A_t}{\ln 2 \times A^0} \tag{13}$$

where A is the ^{90}Sr a activity (Bq), $T_{1.2}$ is the half-life (second), ln 2 is constant number, A_t and A^0 are the mass

Table 2 Liquid scintillation counting (LSC) results for removal and adsorption of ^{90}Sr by CuO NPs/Ag-clinoptilolite zeolite composite under optimized conditions (pH = 8.5, temperature (T = 25 °C) and amount of adsorbent (1.5 g))

Time (h)	CPM (A)	CPM (B)	Activity (Bq/Sample)	Count time min.	MDA (mBq/sample)
0	45065.045	3959.91	110.5	60	6.92
1	9632.90	846.45	23.62		
3	3474.69	317.15	8.52		
6	1272.42	118.8	3.12		
9	1488.57	130.8	3.65		
12	1345.83	118.25	3.30		

number of Sr ($A_t = 90$) and Avogadro's number (g). M is the mass of strontium-90 activity (g).

Kinetics of adsorption reaction

The adsorption kinetics is a significant factor for designing adsorption systems and is required for selecting optimum operating conditions for adsorption reaction study. To investigate the adsorption kinetics of removal of ^{90}Sr by CuO NPs/Ag-clinoptilolite zeolite composite, four different kinetics including models, pseudo first order, pseudo second order, Elovich and intra particle diffusion kinetic, were applied in this study. The pseudo first order Lagergren [42] model presumes that the rate of variation of solute uptake by reaction time is certainly related to versatility in glut concentration and solid uptake value via reaction time (14).

$$\log(q_e - q_t) = \log q_e - 2.303k_1 t \tag{14}$$

where q_e and q_t parameters, are considered as the values of ^{90}Sr which are adsorbed per mass unit of the composite adsorbent ($mg{\cdot}g^{-1}$) at the equilibrium and time t, respectively. k_1 is recognized as the rate constant of the adsorption reaction (min^{-1}). $\log(q_e - q_t)$ was also plotted versus time interval, a straight line should be obtained with a slope of k_1, if the first order kinetics is credible. Ho and McKay [43] proposed a pseudo second order model for the adsorption of divalent metal ions onto sorbent particles that following below Eq. (15):

$$\frac{t}{q_t} = \frac{t}{q_t} + \frac{1}{k_2 q_{e^2}} \tag{15}$$

where q_e and q_t parameters, represent the amount of ^{90}Sr ($g{\cdot}mg^{-1}$) at equilibrium and other time intervals. k_2 is the rate constant of the pseudo second order equation ($g{\cdot}mg^{-1}$ min^{-1}). When the second order model is a suitable expression, a pattern of $\frac{t}{q_t}$ against time (t) will gain a linear result with a slope of $\frac{1}{q}$ and an excise of $\frac{1}{k_2 q_{e^2}}$. The adsorbed amounts (q) of Sr^{2+} were calculated using the following Eq. (16):

$$q = \frac{(C_0 - C_e)V}{m} \tag{16}$$

where C_0 and C_e are the initial and equilibrium concentrations of Sr^{2+} ($g{\cdot}mg^{-1}$) in the liquid phase, respectively, V is the volume of solution (L) and also m is the mass of adsorbent (g). The rate constant of pseudo first order and pseudo second order of the adsorption and correlation coefficient (R^2) were determined from the pattern among $\log(q_e - q_t)$ versus time t and the pattern of t/q versus time t.

Elovich kinetic model

The Elovich equation is represented as it can be observed below (17) [44]:

$$\frac{dq_t}{dt} = \alpha e^{\beta q_t^{-1}} \tag{17}$$

where α and β are considered as the initial sorption rate and the desorption constant both ($mg.g^{-1}$), respectively. The Elovich equation can be simplified if it is presumed that $\alpha\beta t \gg 1$. At the boundary conditions $qt = 0$ at $t = 0$, the above mentioned equation changes to (18) [45]. Plot of Elovich kinetics is given.

$$q_t = \beta \log(\alpha\beta) + \beta \log t \tag{18}$$

Intra particle diffusion model

Each adsorption procedure includes different surface diffusion followed by intra particle diffusion. Generally, the liquid phase mass transport managed the adsorption process. Also the mass transport rate can be imparted as a function of the square root of time (t). As clarified above, the intra particle diffusion model was stated by formula below (19) [45]:

$$q_t = k_i t^{1.2} + C \tag{19}$$

At the above mentioned formula, q_t is the amount of the adsorbed ^{90}Sr on the CuO NPs/Ag-clinoptilolite. Also t and C, are time and intra particle diffusion rate constant,

Table 3 The different kinetics model rate constants for the removal and adsorption of ^{90}Sr on the CuO NPs/Ag-clinoptilolite zeolite composite

Kinetic model	R^2	k_1 (min^{-1})	k_2 ($g.mg^{-1}.min^{-1}$)	k_i ($mmol.mg^{-1}.min^{-1}$)	C	α	β	Plot equation
First order	0.7729	0.1103	–	–	–	–	–	-0.1103×-8.3238
Second order	0.9996	–	7×10^7	–	–	–	–	$7 \times 10^7 \times +9\times10^6$
Elovich	0.8864	–	–	–	–	1.1413	2×10^{-6}	$2 \times 10^{-9} \times +1\times10^{-8}$
Intra particle diffusion	0.6854	–	–	4×10^{-9}	4×10^{-9}	–	–	$4 \times 10^{-9} \times +4\times10^{-9}$

respectively. Plus, the amount of correlation coefficient (R^2) was calculated from the slope and intercept of the drawing of q_t versus $t^{1.2}$. By drawing the plot of q_t versus $t_{1/2}$, it can be obviously inferred that the Sr^{2+} adsorption includes three main steps. First, the analyte ions diffuse among the particles in liquid phase and a rapid adsorption takes place which refers to the Sr^{2+} transfers on the surface active sites of zeolite and then into the porous structure of adsorbent so-called intra particle diffusion. Afterwards, the gradual occupation of active sites slowed down the adsorption of analyte and maintained at a constant value when these active sites were thoroughly saturated. The slight indicated deviations of these lines from the origin specify that the intra particle transportations are not the only rate limiting operative.

The kinetic model along with upper correlation coefficient R^2 was considered as the most appropriate model. Table 3 shows the kinetic factors of the ^{90}Sr adsorption on the CuO NPs/Ag-clinoptilolite. The obtained results illustrates that the R^2 value of pseudo second order kinetic compared to the R^2 value, other kinetics models is higher, thus the ^{90}Sr adsorption on CuO NPs/Ag-clinoptilolite is followed via pseudo second order. The energy of activation E_a calculated by the Arrhenius equation was found to be 44.75 kJ/mol and is expressed as below (20 and 21).

$$k = -A\exp\left(-\frac{E_a}{RT}\right) \tag{20}$$

$$\ln k = -\frac{E_a}{RT} + \mathrm{Ln}A \tag{21}$$

where k is the chemical reaction rate, R is the gas constant (8.314 J mol^{-1} K^{-1}), T is the absolute temperature in kelvin (°K) and A is the pre-exponential factor.

Thermodynamic of removal reaction

Effect of temperature

The temperature in which the experiment fulfills is an important factor that cannot be over looked. In this study, the removal and adsorption of ^{90}Sr on the CuO NPs/Ag-clinoptilolite zeolite composite was surveyed in the temperature scope of 25–50 °C under certain optimized conditions. The spectra of $^{90}Sr/^{90}Y$ and its results are shown in Figs. 9 and 10. Figure 9 illustrates the effect of temperature on the removal of ^{90}Sr on the composite adsorbent surface. As can be seen, the adsorption of ^{90}Sr on the CuO NPs/Ag-clinoptilolite zeolite composite decreases as the temperature increases gradually. The removal reaction efficiency for the temperatures of 25, 30, 35, 40, 45 and 50 °C were 97.17, 90.24, 82.19, 73.72, 60.52 and 41.98 %, respectively. This is why in raised temperatures the formed bonds between ^{90}Sr and active sites of nanoparticles adsorbent will be weaken and broken eventually. The behavior study of the adsorption of ^{90}Sr ions by CuO NPs/Ag-clinoptilolite zeolite composite was investigated as a function of temperature. To determine the process of spontaneous reaction, both important energy and entropy factors should be considered. Moreover, the dependence of distribution ratios on the temperature was evaluated. The relationship between K_d and Gibbs free energy ΔG^0 variation in sorption has been shown below (22):

$$\Delta G = -RT\ln(55.5K_\mathrm{d}) \tag{22}$$

R is the universal gas constant (8.314 J mol^{-1} K^{-1}), T is the absolute temperature in kelvin (°K) and K_d is the distribution coefficient. To gain a correct value of ΔG^0, the K_d value in Eq. (21) must be dimensionless. If the adsorption process was evaluated from an aqueous solution and K_d is considered in dm^3 mol^{-1}, then the parameter K_d can be simply recalculated as dimensionless by multiplying it by 55.5 which refers to the number of moles of water per liter of solution. Therefore, the correct value for ΔG^0 can be gained from the Eq. (21). Thus, the term 55.5 K_d (dm^3 mol^{-1} mol dm^{-3}) is dimensionless [46]. The distribution coefficient was determined at equilibrium in the radioactive solution by the following Eq. (23) [47, 48]:

$$K_\mathrm{d} = \frac{q_\mathrm{e}}{C_\mathrm{e}} = \left(\frac{A_0 - A_\mathrm{e}}{A_\mathrm{e}}\right) \times \frac{V}{m} \tag{23}$$

where A_0 (Bq/L) (or C_0 μmol/L) parameter is the initial strontium activity (or concentration) in solution, A_e (Bq/L) (or C_e μmol/L) parameter is the strontium activity (or concentration) in solution at equilibrium, V (mL) is the solution volume, and m (g) is the adsorbent mass [49].

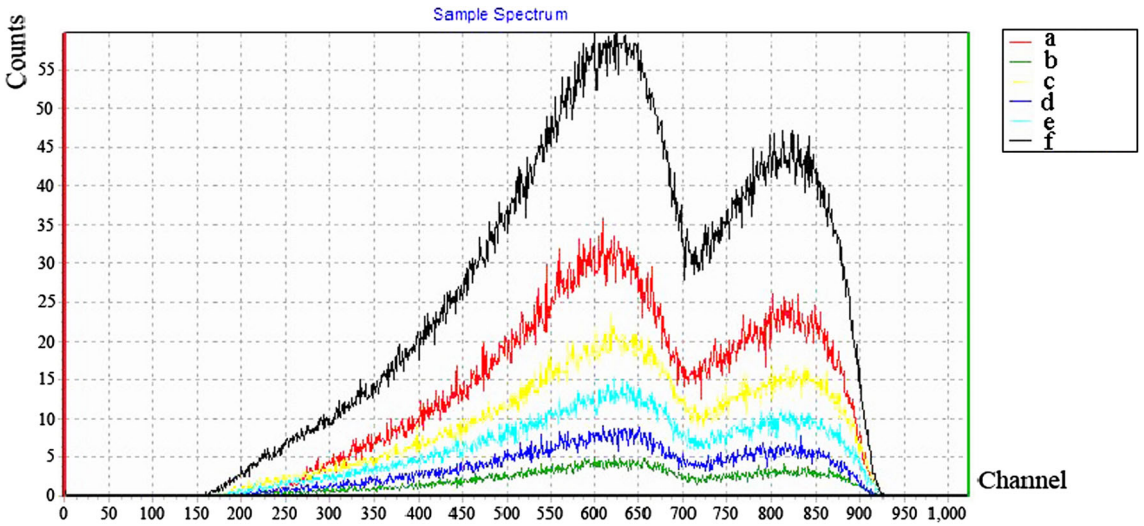

Fig. 9 Liquid scintillation counting (LSC) spectra for removal of ^{90}Sr (count versus channel) at different temperature; **a** 25 °C, **b** 50 °C, **c** 45 °C, **d** 40 °C, **e** 35 °C and **f** 30 °C, under optimized conditions (pH = 8.5, amount of adsorbent (1.5 g) and contact time (6 h))

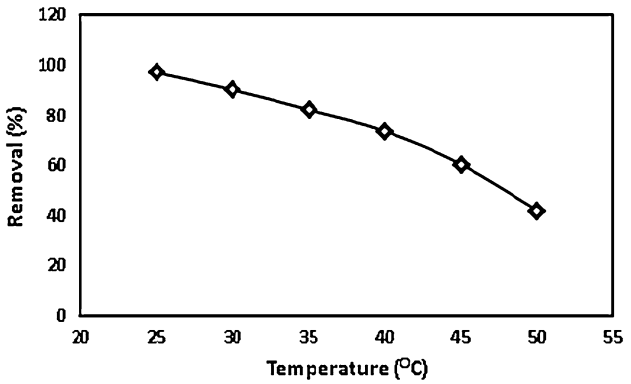

Fig. 10 Plot of ^{90}Sr removal % versus temperature (°C)

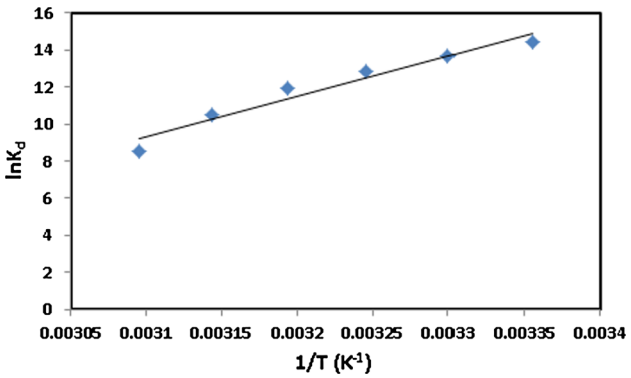

Fig. 11 A plot of vans Hoff (ln K_d versus 1/T) for the removal and adsorption of ^{90}Sr on the CuO NPs/Ag-clinoptilolite zeolite composite at different temperature

Gibbs free energy variation can also be introduced in terms of enthalpy variation, ΔH^0, entropy variation, ΔS^0, as stated in below (24):

$$\Delta G^0 = \Delta H^0 - T\Delta S^0 \tag{24}$$

Besides, by mixing the two above mentioned Eqs. (21–23) a new exposition is attained as is seen in following (Vans Hoff Eq. (25)):

$$lnK_d = -\frac{H^0}{R} \times \frac{1}{T} + \frac{\Delta S^0}{R} \tag{25}$$

The enthalpy (ΔH^0) of adsorption and the entropy (ΔS^0) of adsorption can be specified from the slope and the intercept of the linear fits which are gained by drawing ln K_d against $\frac{1}{T}$ respectively. Also the negative amounts ΔG^0 show that the adsorption procedure is spontaneous with affinity of ^{90}Sr to the composite. Two significant types of adsorption process namely pure physical and pure chemical. During the pure physical adsorption, ΔH^0 values are from 2.1 to 20.9 kJ/mol, while ΔH^0 values corresponded to the pure chemical adsorption are in a ranges 80–200 kJ/mol. ΔH^0 values between 20.9 and 80 kJ/mol related to the physic-chemical adsorption process. The values are well under those related to chemical bond constitution, showing the chemical property of the adsorption process and means that the adsorption of ^{90}Sr on the CuO NPs/Ag-clinoptilolite zeolite composite would be attributed to a chemical adsorption process ($\Delta H^0 = -182.550$ kJ/mol) comparing with above implied information and ranges. Forby, the enthalpy variation ΔH^0 following adsorption is negative in all cases representing the exothermic nature of adsorption that is the removal of ^{90}Sr is decreased as the temperature increases. The entropy variations ΔS^0 of the system along with the adsorption of ^{90}Sr ions on the CuO NPs/Ag-clinoptilolite zeolite composite is positive in all cases showing that more discovery

Table 4 Thermodynamic function values for the removal and adsorption of ^{90}Sr on the CuO NPs/Ag-clinoptilolite zeolite composite

Temperature (°K)	ΔG^0 (KJ/mol)	ΔH^0 (KJ/mol)	ΔS^0 (J/mol K)	R^2	Plot equation
298	−35.816	−182.550	−488.514	0.9523	219578 × −58.758
303	−34.553				
308	−32.895				
313	−31.061				
318	−27.803				
323	−22.896				

is generated following adsorption and reflects that no specific change occurs in the internal structure of composite during adsorption of ^{90}Sr. According to the plots data of ln K_d versus $1/T$ in Fig. 11, the results as shown in Table 4.

The mechanism of Sr^{2+} adsorption on the CuO NPs/Ag-clinoptilolite zeolite composite

The properties such as porosity, presence of alkaline and earth alkaline metallic cations in zeolites structure along with high mechanical and chemical resistance provide good adsorptive, cation exchange, and catalytic characteristics and make them desirable for wide variant of analytical purposes [50, 51]. According to the results reported in this study, the adsorption mechanism of strontium ions on the pre-synthesized CuO NPs/Ag-clinoptilolite zeolite composite adsorbent can be demonstrated by three major possible theories including: (1) the formation of electrostatic or van-der-waals forces of Sr^{2+} with negative charged oxygen and hydroxyl groups originated from zeolite structure on its surface area, (2) the ion exchange process between Sr^{2+} and exchangeable cations (Ag^+, Cu^{2+} and etc.) with negative charge balance of aluminum atoms and (3) the intra porosity diffusion of analyte into the zeolite structure which refers to the above mentioned binding potentials of Sr^{2+} with active sites of zeolite.

Conclusions

This research is focused on the preparation of CuO NPs/Ag-clinoptilolite zeolite composite adsorbent through two facile routes ion exchange and impregnation methods and applied for effective removal of radioactive ^{90}Sr ions from water sample of Bushehr city. The prepared adsorbents were characterized by SEM-EDAX, XRD and FT-IR analyses and the removal process followed via Ultra Low-Level Liquid Scintillation Counting (LSC) as a rapid and suitable analytical technique. Also, different conditions such as pH, amount of adsorbent, the contact time and temperature were investigated and optimized to approach the highest adsorption/removal efficiency of strontium-90. Moreover, Adsorption isotherms including Langmuir, Freundlich, Temkin, D-R, H-J and Hasley have been analyzed to the equilibrium data. The Freundlich, Temkin, H-J and Hasley isotherms were found good to represent the measured adsorption data. The parameters including: pH = 8.5, amount of adsorbent (1.5 g), contact time (6 h) and temperature (25 °C) were considered as optimized conditions for this process. The experimental results denoted that CuO NPs/Ag-clinoptilolite zeolite composite leads to maximum removal and adsorption of ^{90}Sr from water sample. On the other hand, the reaction kinetic information was surveyed utilizing pseudo first and second orders, Elovich and Intra particle diffusion kinetic models. Besides, the adsorption kinetics of ^{90}Sr was matched nicely with the pseudo second order kinetic model. Then, thermodynamic study for the adsorption reactions was evaluated and the results showed that by increasing the temperature, efficiency reaction decreased. It was emphasized that CuO NPs/Ag-clinoptilolite zeolite composite has a high capacity and potential for the removal of radioactive ^{90}Sr from water sample. It should be noted that the presented composite adsorbent as a potentially applicable adsorbent can be considered for further analytical procedures in future.

Acknowledgments The authors give their sincere thanks to the Islamic Azad University, Ahvaz, Iran, Islamic Azad University, Qaemshahr, Iran and Islamic Azad University, Bushehr, Iran for all their supports.

References

1. Sachse A, Merceille A, Barre Y, Grandjean A, Fajula F, Galarneau A (2012) Macroporous LTA-monoliths for in-flow removal of radioactive Sr^{2+} from aqueous effluents: application to the case of Fukushima. Macropo Mesopo Mater 164:251–258

2. Hari P, Bimala P, Inoue Katsutoshi, Ohto Keisuke, Kawakita Hidetaka, Kedar NG, Hiroyuki H, Shafiq A (2014) Adsorptive removal of strontium from water by using chemically modified orange juice residue. Separat Sci Technol 49:1244–1250
3. Mashkani SG, Ghazvini PTM (2009) Biotechnological potential of Azolla filiculoides for biosorption of Cs^{+} and Sr^{2+}: application of micro-PIXE for measurement of biosorption. Biores Technol 100:1915–1921
4. Carboneau ML, Adams JP, Garcia RS (1994) National low-level waste management program radionuclide report series, vol. 7: Strontium-90. Idaho National Engineering Laboratory, Idaho Falls
5. Sebesta F, Motl John AJ (1993) Proceedings of International Conference on Nuclear Waste Management and Environmental Remediation, Prague, 3, p 871
6. Mardan A, Ajaz R, Mehmood A, Raza SM, Ghaffar A (1999) Preparation of silica potassium cobalt hexacyanoferrate composite ion exchanger and its uptake behaviour for cesium. Sep Purif Technol 16:147–158
7. Murthy ZVP, Parmar S (2011) Removal of Sr^{2+} by electrocoagulation using stainless steel and aluminium electrode. Desalination 282:63–67
8. Bascetin E, Atun G (2010) Adsorptive removal of Sr^{2+} by binary mineral mixtures of montmorillonite and zeolite. J Chem Eng Data 55:783–788
9. Chegrouche S, Mellah A, Barkat M (2009) Removal of Sr^{2+} from aqueous solutions by adsorption onto activated carbon: kinetic and thermodynamic studies. Desalination 235:306–318
10. Ghaemi A, Mostaidi MT, Maragheh MG (2011) Charecterization of Sr^{2+} and Ba^{2+} adsorption from aqueous solutions using dolomite powder. J Hazard Mater 190:916–921
11. Hossein F, Mozhgan I, Mohammad M, Mohammad GM (2013) Preparation of a novel PAN–zeolite nanocomposites for removal of Cs^{+} and Sr^{2+} from aqueous solutions: kinetic equilibrium, and thermodynamic studies. Chem Eng J 222:41–48
12. Hossein F, Mohammad M, Alireza F, Mozhgan I (2013) Synthesis of a novel magnetic zeolite nanocomposites for removal of Cs^{+} and Sr^{2+} from aqueous solution: kinetic, equilibrium, and thermodynamic studies. J Colloid Interface Sci 393:445–451
13. Saheed SO, Modise SJ, Sipalma AM (2013) TiO_2 supported clinoptilolite characterization and optimization of operational parameters for methyl orange removal. Adv Mater Res 781–784:2249–2252
14. Mohammad A (2014) Khakizadeh, Hoda Keipour, Abolfazl Hosseini, Daryoush Zareyee, KF/clinoptilolite, an effective solid base in Ullmann ether synthesis catalyzed by CuO nanoparticles. New J Chem 38:42–45
15. Jahangirian H (2013) Synthesis and characterization of zeolite/Fe_3O_4 nanoparticle by green quick precipitation method. Dig J Nanomater Bios 8:1405–1413
16. Yusan S, Erenturk S (2011) Adsorption characterization of strontium on PAN/zeolite composite adsorbent. World J Nucl Sci Technol 1:6–12
17. Huang Y, Wang W, Feng Q, Dong F (2013) Preparation of magnetic clinoptilolite/$CoFe_2O_4$ composites for removal of Sr^{2+} from aqueous solutions: kinetic, equilibrium, and thermodynamic studies. J Saudi Chem Soc 09:1–9
18. Dastafkan K, Sadeghi M, Obeydavi A (2014) Manganese dioxide nanoparticles-silver-Y zeolite as a nanocomposite catalyst for the decontamination reactions of O, S-diethyl methyl phosphonothiolate. Int J Environ Sci Technol. doi:10.1007/s13762-014-0701-1
19. Sadeghi M, Hosseini MH (2013) The detoxification of methamidophos as an organophosphorus insecticide on the magnetite (Fe_3O_4) nanoparticles/Ag-NaY faujasite molecular sieve zeolite (FMSZ) composite. Int J Bio-Inorg Hybd Nanomat 2:517–524
20. Buarod E, Pithakratanayothin S, Naknaka S, Chaiyasith P, Yotkaew T, Tosangthumb N, Tongsri R (2015) Facile synthesis and characterization of tenorite nanoparticles from gas-atomized Cu powder. Powder Technol 269:118–126
21. Engelbrekt C, Malcho P, Andersen J, Zhang L, Stahl Bin Li K, Hu J, Zhang JD (2014) Selective synthesis of clinoatcamite $Cu_2(OH)_2Cl$ and tenorite CuO nanoparticles by pH control. J Nanopart Res 16:2562–2564
22. Yin M, Wu CK, Lou Y, Burda C, Koberstein JT, Zhu Y, O'Brien S (2005) Copper oxide nanocrystals. J Am Chem Soc 127:9506–9511
23. Shaffiey SF, Shapoori M, Bozorgnia A, Ahmadi M (2014) Synthesis and evaluation of bactericidal properties of CuO nanoparticles against Aeromonas hydrophila. Nanomed J 1:198–204
24. Salavati-Niasari M, Davar F (2009) Synthesis of copper and copper (I) oxide nanoparticles by thermal decomposition of a new precursor. Mater Lett 63:441–443
25. Sadeghi M, Ghaedi H, Yekta S, Babanezhad E (2016) Decontamination of toxic chemical warfare sulfur mustard and nerve agent simulants by NiO NPs/Ag-clinoptilolite zeolite composite adsorbent. J Environ Chem Eng 4:2990–3000
26. Sadeghi M, Hosseini MH (2012) Preparation and application of MnO_2 nanoparticles/zeolite AgY composite catalyst by confined space synthesis (CSS) method for the desulfurization and elimination of SP and OPPJ. Nano Struct 2:439–453
27. Abdi MR, Shakur HR, Rezaee Ebrahim Saraee Kh, Sadeghi M (2014) Effective removal of uranium ions from drinking water using CuO/X zeolite based nanocomposites: effects of nano concentration and cation exchange. J Radioanal Nucl Chem 300(3):1217–1225. doi:10.1007/s10967-014-3092-3
28. Lou LL, Liu S (2005) CuO-containing MCM-48 as catalysts for phenol hydroxylation. Catal Commun 6:762–765
29. Li Z, Gao L (2003) Synthesis and characterization of MCM-41 decorated with CuO particles. J Phys Chem Solids 64:223–228
30. Hao XY, Zhang YQ, Wang JW, Zhou W, Zhang C, Liu S (2006) A novel approach to prepare MCM-41 supported CuO catalyst with high metal loading and dispersion. Microporous Mesoporous Mater 88:38–47
31. Debye P, Scherrer P (1916) The Scherrer equation versus the 'Debye-Scherrer equation'. Phys Z 17:277–283
32. Langmuir I (1916) The constitution and fundamental properties solids and liquids. J Am Chem Soc 38:2221–2225
33. Freundlich HMF (1906) User die adsorption in losungen. Z Phys Chem 57:385–470
34. Temkin MI (1941) Adsorption equilibrium and kinetics of processes on non-homogeneous surface and in the interaction between adsorbed molecules. Zh Fiz Chim 15:296–332
35. Foo KY, Hamed BH (2010) Insight into modeling of adsorption isotherm systems. Chem Eng J 156:2–10
36. Hasley GD (1952) The role of surface heterogeneity. Adv Catal 4:259–267
37. Abadzic SA, Ryan JN (2001) Particle release and permeability reduction in a natural zeolite (clinoptilolite) porous medium. Environ Sci Technol 35:4502–4508
38. Yavari R, Huang YD, Mostofizadeh A (2010) Sorption of strontium ions from aqueous solutions by oxidized multiwall carbon nanotubes. J Radioanal Nucl Chem 285:703–710
39. Talaie N, Aghabozorg HR, Alamdar Milani S (2012) Cs and Sr absorption study using synthesized titanosilicate nanoparticles, containing Nb and Ge, Proceedings of the 4th International Conference on Nanostructures (ICNS4) 12–14 March, Kish Island, IR Iran
40. Sadeghi M, Yekta S, Ghaedi H, Babanezhad E (2015) Synthesis and characterization of γ-MnO_2-AgA zeolite nanocomposite and its application for the removal of radioactive strontium-90 (^{90}Sr) Int. J Bio-Inorg Hybr Nanomater 4:101–111

41. Currie LLA (1968) Limits for qualitative detection and quantitative determination. Anal Chem 40:586–593
42. Lagergern S (1898) About the theory of so-called adsorption of soluble substances. K Sven Vetenskapsakad Handl 24:1–39
43. Mckay YSG (1998) The kinetics of sorption of basic dyes from aqueous solution by sphagnum moss peat. Can J Chem Eng 76:822–827
44. Liang S, Guo X, Feng N, Tian Q (2010) Isotherms, kinetics and thermodynamic studies of adsorption of Cu^{2+} from aqueous solutions by Mg^{2+}/K^{+} type orange peel adsorbents. J Hazard Mater 174:756–762
45. Annadurai G, Juang RS, Lee DJ (2002) Use of cellulose-based wastes for adsorption of dyes from aqueous solutions. J Hazard Mater 92:263–274
46. Milonjić SK (2007) A consideration of the correct calculation of thermodynamic parameters of adsorption. J Serb Chem Soc 72(12):1363–1367
47. Merceille A, Weinzaepfel E, Barre Y, Grandjean A (2012) The sorption behavior of synthetic sodium nonatitanate and zeolite A for removing radioactive strontium from aqueous wastes. Sep Purif Technol 96:81–88
48. Nishiyama Y, Hanafusa T, Yamashita J, Yamamoto Y, Ono T (2016) Adsorption and removal of strontium in aqueous solution by synthetic hydroxyapatite. J Radioanal Nucl Chem 307(2):1279–1285. doi:10.1007/s10967-015-4228-9
49. Lívia K, Lima S, Jean F, Silva L, Meuris G, da Silva C, Melissa G, Vieira A (2014) Lead biosorption by salvinia natans biomass: equilibrium study. Chem Eng Trans 38:97–102. doi:10.3303/CET1438017
50. Perić J, Trgo M, Vukojević Medvidović N (2004) Removal of zinc, copper and lead by natural zeolite-a comparison of adsorption isotherms. Water Res 38(7):1893–1899
51. Ersoy B, Çelik MS (2003) Effect of hydrocarbon chain length on adsorption of cationic surfactants onto clinoptilolite. Clays Clay Miner 51(2):172–180